

1 **How the replication and transcription complex**
2 **functions in jumping transcription of SARS-CoV-2**

3 Jianguang Liang^{1§}, Jinsong Shi^{2§}, Shunmei Chen³, Guangyou Duan⁴, Fan Yang²

4 Zhi Cheng⁵, Xin Li⁵, Jishou Ruan⁶, Dong Mi^{7*}, Shan Gao^{5*}

5 ¹ School of Pharmacy, Changzhou University, Changzhou, Jiangsu 213164, P. R. China;

6 ² National Clinical Research Center of Kidney Disease, Jinling Hospital, Nanjing University
7 School of Medicine, Nanjing, Jiangsu 210016, P. R. China;

8 ³ Yunnan Key Laboratory of Stem Cell and Regenerative Medicine, Biomedical Engineering
9 Research Center, Kunming Medical University, Kunming, Yunnan 650500, P. R. China;

10 ⁴ School of Life Sciences, Qilu Normal University, Jinan, Shandong 250200, P. R. China;

11 ⁵ College of Life Sciences, Nankai University, Tianjin, Tianjin 300071, P. R. China;

12 ⁶ School of Mathematical Sciences, Nankai University, Tianjin, Tianjin 300071, P. R. China;

13 ⁷ Department of Clinical Laboratory, Tianjin Central Hospital of Obstetrics and Gynecology,
14 Affiliated Maternity Hospital, Nankai University, Tianjin 300100, P. R. China.

15

16

17

18

19 [§] These authors contributed equally to this paper.

20 * Corresponding authors.

21 SG: gao_shan@mail.nankai.edu.cn

22 DM: mrmidong@163.com

23

24 **Abstract**

25 **Background:** Coronavirus disease 2019 (COVID-19) is caused by severe acute
26 respiratory syndrome coronavirus 2 (SARS-CoV-2). Although unprecedented efforts
27 are underway to develop therapeutic strategies against this disease, scientists have
28 acquired only a little knowledge regarding the structures and functions of the CoV
29 replication and transcription complex (RTC) and 16 non-structural proteins, named
30 NSP1-16.

31 **Results:** In the present study, we proposed a two-route model to answer how the RTC
32 functions in the jumping transcription of CoVs. The key step leading to this model
33 was that the motif AAACH for METTL3 recognition flanking the transcription
34 regulatory sequence (TRS) motif was discovered to determine the m6A methylation
35 of SARS-CoV-2 RNAs, by reanalyzing public Nanopore RNA-seq data. As the most
36 important finding, TRS hairpins were reported for the first time to interpret NSP15
37 cleavage, RNA methylation of CoVs and their association at the molecular level. In
38 addition, we reported canonical TRS motifs of all CoVs to prove the importance of
39 our findings.

40 **Conclusions:** The main conclusions are: (1) TRS hairpins can be used to identify
41 recombination regions in CoV genomes; (2) RNA methylation of CoVs participates in
42 the determination of the RNA secondary structures by affecting the formation of base
43 pairing; and (3) The eventual determination of the CoV RTC global structure needs to
44 consider METTL3 in the experimental design. Our findings enrich fundamental
45 knowledge in the field of gene expression and its regulation, providing a crucial basis
46 for future studies.

47 **Keyword:** Coronavirus; Jumping transcription; RNA methylation; Nanopore;
48 TRS hairpin

49

50 Introduction

51 Coronavirus disease 2019 (COVID-19) is caused by severe acute respiratory
52 syndrome coronavirus 2 (SARS-CoV-2) [1] [2] with a genome of ~30 kb [3]. By
53 reanalyzing public data [4], we determined that a SARS-CoV-2 genome has 12 genes,
54 which are *spike (S)*, *envelope (E)*, *membrane (M)*, *nucleocapsid (N)*, and *ORF1a, 1b*,
55 *3a, 6, 7a, 7b, 8* and *10*. The *ORF1a* and *1b* genes encode 16 non-structural proteins
56 (NSPs), named NSP1 through NSP16 [5], while the other 10 genes encode 4
57 structural proteins (S, E, M and N) and 6 accessory proteins (ORF3a, 6, 7a, 7b, 8 and
58 10). Among the above 26 proteins, NSP4-16 are significantly conserved in all known
59 CoVs and have been experimentally demonstrated or predicted to be critical enzymes
60 in CoV RNA synthesis and modification [6], particularly including: NSP12,
61 RNA-dependent RNA polymerase (RdRp) [7]; NSP13, RNA helicase-ATPase (Hel);
62 NSP14, RNA exoribonuclease (ExoN) and N7 methyltransferase (MTase); NSP15
63 endoribonuclease (EndoU) [8]; and NSP16, RNA 2'-O-MTase.

64 NSP1-16 assemble into a replication and transcription complex (RTC) in CoV
65 [7]. The basic function of the RTC is RNA synthesis: it synthesizes genomic RNAs
66 (gRNAs) for replication or transcription of the *ORF1a, 1b* genes, while it synthesizes
67 subgenomic RNAs (sgRNAs) for jumping transcription of the other 10 genes [4]. In
68 1998, the “leader-to-body fusion” model [9] was proposed to explain the jumping
69 transcription, however, the molecular basis of this model was unknown until our
70 previous study in 2020 [10]. For a complete understanding of CoV replication and
71 transcription, particularly the jumping transcription, much research [7] [8] [11] has
72 been conducted to determine the global structure of the SARS-CoV-2 RTC, since the
73 outbreak of SARS-CoV-2. Although some single protein structures (e.g. NSP15 [8])
74 and local structures of the RTC (i.e. NSP7&8&12&13 [7] and NSP7&8&12 [11])
75 have been determined, there will be a long way to completely understand how the
76 RTC functions in the jumping transcription at the molecular level. As the global

77 structure of the CoV RTC cannot be determined by simple use of any current methods
78 (i.e., NMR, X-ray and Cryo-EM), it is necessary to ascertain all the RTC components
79 and the arrangement of them, leading to the eventual determination of its global
80 structure and the complete understanding all of its functions at the molecular level.

81 In our previous study, we provided a molecular basis for the “leader-to-body
82 fusion” model by identifying the cleavage sites of NSP15 and proposed a negative
83 feedback model to explain the regulation of CoV replication and transcription. In
84 addition, we revealed that the jumping transcription and recombination of CoVs share
85 the same molecular mechanism [10], which inevitably causes CoV outbreaks. These
86 findings are vital for the further investigation of CoV transcription and recombination.
87 In the present study, we aimed to determine the theoretical arrangement of NSP12-16
88 in the global structure of the CoV RTC by comprehensive analysis of data from
89 different sources, and to elucidate how the RTC functions in the jumping transcription
90 of CoVs at the molecular level.

91

92 **Results**

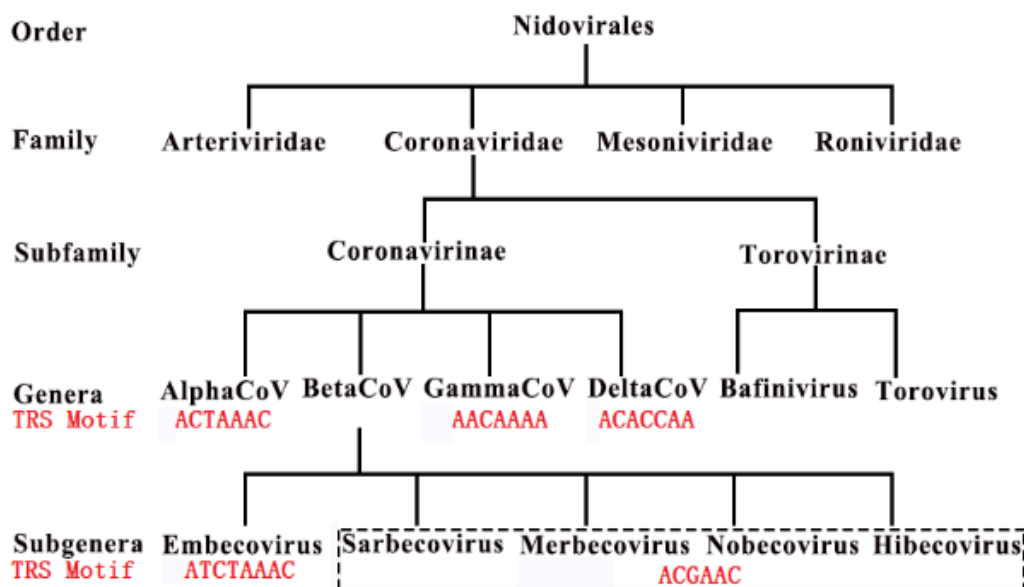
93 **Molecular basis of “leader-to-body fusion” model**

94 Here, we provide a brief introduction to the “leader-to-body fusion” model
95 proposed in an early study [9] and its molecular basis proposed in our recent study
96 [10]. CoV replication and transcription require gRNAs(+) as templates for the
97 synthesis of antisense genomic RNAs [gRNAs(-)] and antisense subgenomic RNAs
98 [sgRNAs(-)] by RdRP. When RdRP pauses, as it crosses a body transcription
99 regulatory sequence (TRS-B) and switches the template to the leader TRS (TRS-L),
100 sgRNAs(-) are formed through jumping transcription (also referred to as
101 discontinuous transcription, polymerase jumping or template switching). Otherwise,
102 RdRP reads gRNAs(+) continuously, without interruption, resulting in gRNAs(-).
103 Thereafter, gRNAs(-) and sgRNAs(-) are used as templates to synthesize gRNAs(+)

104 and sgRNAs(+), respectively; gRNAs(+) and sgRNAs(+) are used as templates for the
 105 translation of NSP1-16 and the other 10 proteins (S, E, M, N, and ORF3a, 6, 7a, 7b, 8
 106 and 10), respectively. The molecular basis of the “leader-to-body fusion” model as
 107 proposed in our previous study is that NSP15 cleaves gRNAs(-) and sgRNAs(-) at
 108 TRS-Bs(-). Then, the free 3' ends (~6 nt) of TRS-Bs(-) hybridize TRS-Ls to realize
 109 “leader-to-body fusion”. NSP15 may also cleave gRNAs(-) and sgRNAs(-) at
 110 TRS-Ls(-), which is not necessary for jumping transcription.

111 The NSP15 cleavage of TRS-Bs(-) and their fusion to the TRS-L require a
 112 sequence motif, named TRS motif. We defined the TRS motif in the TRS-L as the
 113 canonical TRS motif. Thus, the canonical TRS motif is unique to a CoV genome,
 114 while the TRS motifs in TRS-Bs can be canonical TRS motifs or non-canonical TRS
 115 motifs with little nucleotide differences. In our previous study [10], we found that a
 116 TRS motif is a 6~8 nucleotide sequence (only for CoVs) beginning with at least an
 117 adenosine residue (A), while its antisense sequence is a NSP15 cleavage site.

118



119

120 **Figure 1 Canonical TRS hairpins in Coronaviridae Embecovirus, Sarbecovirus,**
 121 *Merbecovirus, Nobecovirus* a defined as subgroups A, B, C, D and E. The present
 122 study TRS motifs (in red color) of viruses in Coronaviridae.

123

124 For example, the canonical TRS motif and NSP15 cleavage site of SARS-CoV-2 is
125 ACGAAC and GTTCGT, respectively. The discovery of NSP15 cleavage made it
126 possible to eventually determine canonical TRS motifs of all CoVs (**Figure 1**) and
127 corrected some canonical TRS motifs reported in the previous studies. For example,
128 the canonical TRS motifs of mouse hepatitis virus (MHV), transmissible
129 gastroenteritis virus (TGEV), Canada goose coronavirus (Goose-CoV) and beluga
130 whale coronavirus (BWCoV) were corrected from CTAAAC [12], CTAAAC [13],
131 CTTAACAAA [14] and AAACA [15] to ATCTAAAC, ACTAAAC, AACAAA and
132 AACAAA, respectively. Canonical TRS motifs are highly conserved in
133 Alphacoronavirus, Gammacoronavirus, Deltacoronavirus and Betacoronavirus except
134 the subgroup A (**Figure 1**). Betacoronavirus subgroup A has the canonical TRS motif
135 ATCTAAAC, which is different from ACGAAC of subgroup B, C, D and E.
136 Different from Betacoronavirus B, Betacoronavirus subgroup A, C, D and E,
137 Alphacoronavirus, Gammacoronavirus and Deltacoronavirus have non-canonical TRS
138 motifs in TRS-Bs of 4 structural genes (*S*, *E*, *M* and *N*), which were caused by
139 mutations. These TRS motif mutations down-regulate the transcription of CoV genes
140 except *ORF1a* and *1b*, then resulted in the attenuation of CoVs from subgroup A, D
141 and E during evolution [16]. Therefore, Betacoronavirus subgroup B will pose the
142 greatest threat to humans and animals for a long period.

143

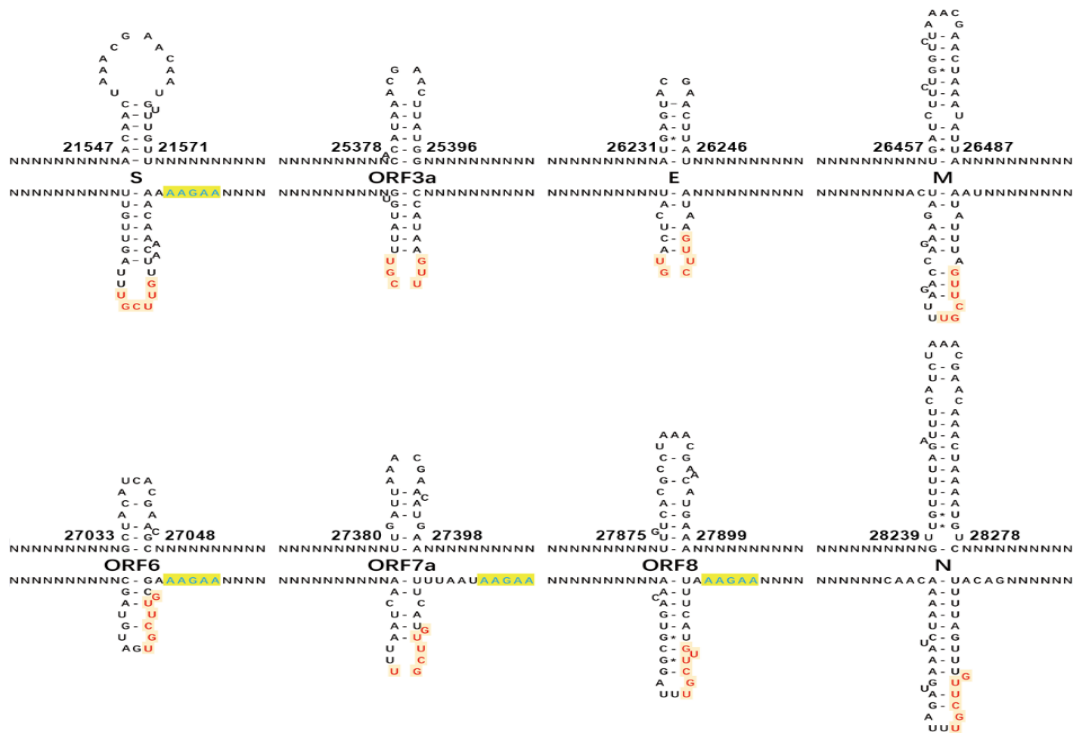
144 **RNA methylation, NSP15 cleavage and TRS hairpins**

145 A previous study reported that RNA methylation sites contain the “AAGAA-like”
146 motif (including AAGAA and other A/G-rich sequences) throughout the
147 SARS-CoV-2 genome, particularly enriched in genomic positions 28,500-29,500 [4].
148 This study used Nanopore RNA-seq, a direct RNA sequencing method [17], which
149 can be used to measure RNA methylation at 1-nt resolution although it has a high
150 error rate. By analyzing the Nanopore RNA-seq data [4], a preliminary comparison in
151 the previous study [4] was conducted for a new finding that methylated RNAs of

152 SARS-CoV-2 have shorter 3' polyA tails than methylated ones. Although the type of
153 the RNA methylation was unknown, the previous study [4] concluded that the
154 “AAGAA-like” motif associates with the 3' polyA lengths of gRNAs and sgRNAs,
155 which merits further analysis. However, there were three shortcomings in the study:
156 (1) it was not explained that many internal methylation sites are far from 3' ends,
157 which are unlikely to contribute to the 3' polyA lengths; (2) since only a few antisense
158 reads were obtained using Nanopore RNA-seq, the previous study should have
159 analyzed but did not analyze the “AAGAA-like” motif on the antisense strand (**See**
160 **below**), particularly the association between the “AAGAA-like” motif and the TRS
161 motif; and (3) based on their explanation, the methylation at the “AAGAA-like” motif
162 may also affect the downstream 3' polyadenylation of the antisense nascent RNAs that
163 prevents the quick degradation of them, which is not supported by the extremely high
164 ratio between sense and antisense reads [10].

165 Our analysis of the SARS-CoV-2 genome revealed that the “AAGAA-like”
166 motif co-occurred with the TRS motif ACGAAC in TRS-Bs of eight genes (*S*, *E*, *M*,
167 *N*, and *ORF3a*, *6*, *7a* and *8*). In addition, we found the association between the
168 “AAGAA-like” motif and the TRS motif through the discovery of hairpins in these
169 TRS-Bs (**Figure 2**). These hairpins are encoded by complemented palindrome
170 sequences, which explained a finding reported in our previous study [18]:
171 complemented palindromic small RNAs (cpsRNAs) with lengths ranging from 14 to
172 31 nt are present throughout the SARS-CoV genome, however, most of them are
173 semipalindromic or heteropalindromic. In the present study, we defined: (1) the
174 hairpins containing the canonical and non-canonical TRS motifs are canonical and
175 non-canonical TRS hairpins, respectively; and (2) the hairpins opposite to the TRS
176 hairpins as the opposite TRS hairpins (**Figure 2**). The formation of these opposite
177 TRS hairpins is uncertain, as all the complemented palindrome sequences in the TRS
178 hairpins and opposite TRS hairpins are asymmetric (semipalindromic or
179 heteropalindromic). By analyzing the junction regions between TRS-Bs and the

180



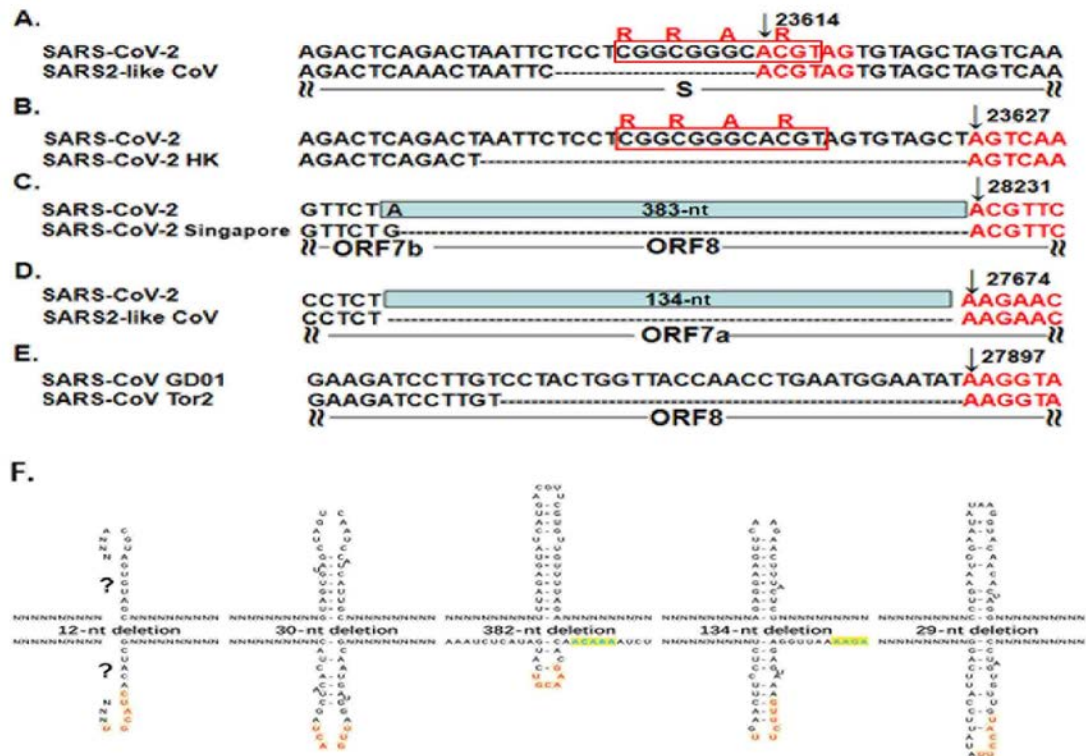
181

182 **Figure 2 Canonical TRS hairpins in SARS-CoV-2** (The canonical transcription
 183 regulatory sequence (TRS) motif ACGAAC is present in TRS-Bs of eight genes (S, E,
 184 M, N, and ORF3a, 6, 7a and 8). Read on the antisense strands of the SARS-CoV-2
 185 genome (GenBank: MN908947.3), “AAGAA” (in blue color) and “GUUCGU” (in
 186 red color) represent RNA methylation sites and NSP15 cleavage sites, respectively.
 187 The positions are the start and end positions of hairpins in the SARS-CoV-2 genome.
 188 NSP15 cleave the single RNA after U (indicated by arrows). In the present study, we
 189 defined: (1) the hairpins containing the canonical and non-canonical TRS motifs are
 190 canonical and non-canonical TRS hairpins, respectively; and (2) the hairpins opposite
 191 to the TRS hairpins as the opposite TRS hairpins.)

192

193 TRS-L of SARS-CoV-2, we found that NSP15 cleaves the canonical TRS hairpin of
 194 *ORF3a* at an unexpected breakpoint “GTTCGTTTTAT|N” (the TRS motif is
 195 underlined; the vertical line indicates the breakpoint and N represents any nucleotide
 196 base), rather than the end of the canonical TRS motif “GTTCGTTTTATN”. Here, we
 197 defined the breakpoints “GTTCGTTTTATN” and “GTTCGTTTTAT|N” as canonical
 198 and non-canonical TRS breakpoints, respectively. The discovery of non-canonical
 199 TRS hairpins and non-canonical TRS breakpoints in many non-canonical junction
 200 regions [10] indicated that the recognition of NSP15 cleavage sites is structure-based

201 rather than sequence-based. Then, we validated that non-canonical TRS hairpins are
 202 present in seven common recombination regions which were reported as RC1 to RC7
 203 by analyzing 292 genomes of betacoronavirus subgroup B (**Materials and Methods**)
 204 in our previous study [16]. Non-canonical TRS hairpins are also present in five
 205 recombination events (**Figure 3**) which were analyzed in our previous study [10].
 206



207
 208 **Figure 3 TRS hairpins in five recombination regions**(A-E have already been
 209 published in our previous study [10]. N represents any nucleotide base. All the
 210 positions were annotated on the SARS-CoV (GenBank: AY278489) or SARS-CoV-2
 211 (GenBank: MN908947) genomes. **A.** The genome (GenBank: MN996532) of the
 212 SARS2-like CoV strain RaTG13 from bats is used to show the 12-nt deletion; **B.** The
 213 genome (GISAID: EPI_ISL_417443) of the SARS-CoV-2 strain Hongkong is used to
 214 show the 30-nt deletion; **C.** The genomes (GISAID: EPI_ISL_414378,
 215 EPI_ISL_414379 and EPI_ISL_414380) of three SARS-CoV-2 strains from
 216 Singapore are used to show the 382-nt deletion; **D.** The genome (GenBank:
 217 MT457390) of the mink SARS2-like CoV strain is used to show the 134-nt deletion;
 218 **E.** The genome (GenBank: AY274119) of the SARS-CoV strain Tor2 is used to show
 219 the 29-nt deletion;. **F.** These recombinant events occurred at the non-canonical TRS
 220 motifs that also begin with at least an adenosine residue (“A”), due to the cleavage of
 221 the non-canonical TRS hairpins.)

222

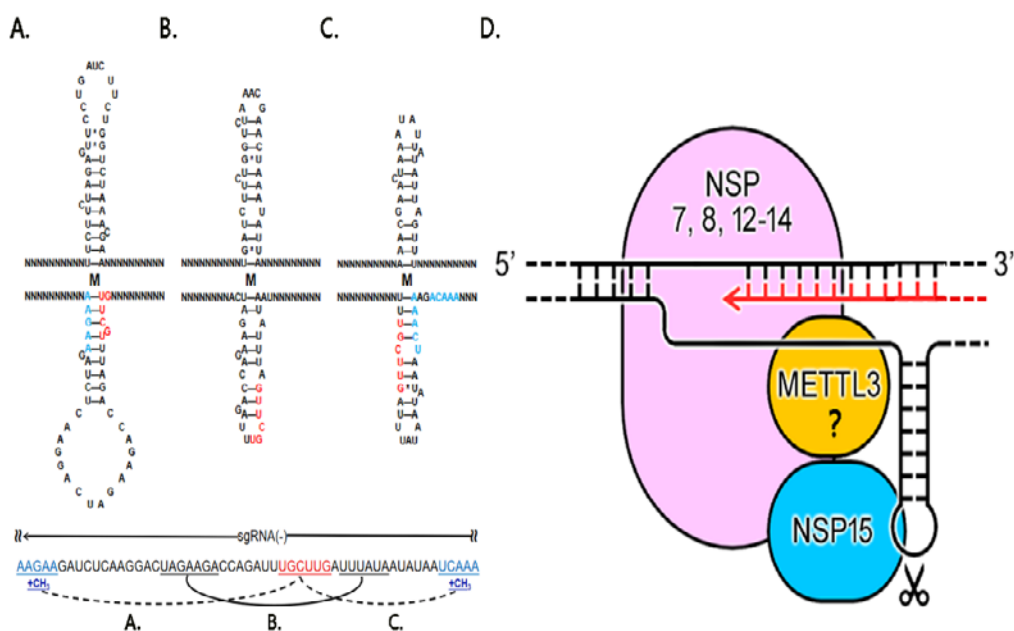
223 Therefore, TRS hairpins can be used to identify recombination regions in CoV
224 genomes. More importantly, we found the association between RNA methylation and
225 NSP15 cleavage by analyzing TRS hairpins.

226

227 **How RTC functions in jumping transcription**

228 Since several A-rich and T-rich regions are alternatively present in each TRS-B,
229 each TRS-B contains many possible hairpins (**Figure 4ABC**). Thus, to investigate if a
230 unique TRS hairpin can be formed needs a further analysis of the association between
231 the “AAGAA-like” motif and the TRS motif. After comparing all possible hairpins in
232 the TRS-Bs of betacoronavirus subgroup B, we found that they can be classified into
233 three types. Using the *M* gene of SARS-CoV-2 as an example, the minimum free
234 energies (MFEs) of three possible hairpins containing the TRS motif were estimated
235 as -2.50, -4.00 and -4.90 kcal/mol (**Materials and Methods**). Although the third
236 hairpin (**Figure 4C**) is the most stable one, the differences of MFEs between the
237 second (**Figure 4B**) of third possible hairpins are still small. The first (**Figure 4A**)
238 and the third hairpins (**Figure 4C**) require the “AAGAA-like” and “AAACH” motifs
239 (**See below**) involved in the base pairing, respectively. However, RNA methylation of
240 specific types (e.g., m6A) is not in favour of base pairing, in our view. Further
241 analysis of the “AAGAA-like” and “AAACH” motifs on the antisense strand inspired
242 us to propose a novel interpretation of RNA methylation. RNA methylation of CoVs
243 participates in the determination of the RNA secondary structures by affecting the
244 formation of base pairing. The methylation of flanking sequences containing the
245 “AAGAA-like” or “AAACH” motif ensures the formation of a unique stable hairpin
246 as the TRS hairpin in all likelihood. In the unique hairpin, the NSP15 cleavage site
247 exposes in a small loop, which facilitates the contacts of NSP15, while the loop of the
248 opposite TRS hairpin may not contain uridine residues (**Figure 4 B**). This structure
249 verified the results of mutation experiments in a previous study [19] that the

250 recognition of NSP15 cleavage sites is independent on the TRS motif, but dependent
 251 on its context. These findings confirmed that the recognition of NSP15 cleavage sites
 252 is structure-based (TRS hairpin) rather than sequence-based (TRS motif). By
 253 comprehensively analyzing the associations between the “AAGAA-like”, “AAACH”
 254 motifs, the TRS motifs and the TRS hairpins (**Figure 4A-C**), we proposed that the
 255 RTC has a local structure that facilitates the NSP15 cleavage of the TRS hairpin
 256 (**Figure 4D**).
 257



258
 259 **Figure 4 How RTC functions in jumping transcription** (N represents any
 260 nucleotide base. All possible hairpins in the TRS-Bs were classified into three types.
 261 Using the *M* gene of SARS-CoV-2 as an example, the first type (A) and the third type
 262 (C) require the “AAGAA-like” or AAACH motifs involved in the base pairing.
 263 However, the m6A methylation of “AAGAA” and “AAACU” (in blue color) is not in
 264 favour of base pairing, which ensures a unique stable hairpin containing the NSP15
 265 cleavage site in the loop (B). This is the TRS hairpin. (D) 5'-3' represents the strand of
 266 the SARS-CoV-2 genome. RTC processes the double strand RNAs (dsRNAs) and
 267 single strand RNAs (ssRNAs) in two routes. Nascent RNAs are synthesized in the
 268 first route. RNSP15 cleaves the single RNA at the TRS motif in a small loop in the
 269 second route.)
 270

271 The above findings addressed another important topic: which enzyme is
272 responsible for the internal methylation of CoV RNAs that is supposed to be done
273 before the NSP15 cleavage for jumping transcription. A recent study reported that
274 NSP14 (no structure data available) and NSP10&16 (PDB: 7BQ7), as N7 and
275 2'-O-MTase respectively (**Introduction**), are crucial for RNA cap formation [23].
276 This suggested that NSP14 and NSP10&16 are unlikely to function in the internal
277 methylation of CoV RNAs. Thus, NSP10&16 may be not included in the main
278 structure of the RTC. Although the previous study excluded METTL3-mediated m6A
279 (for lack of canonical motif RRACH) [4], we still found the internal methylation sites
280 “agTtt” (the underlined capital letter) at the positions 29408 and 29444, and “tgTtt” at
281 the position 29170 in the SARS-CoV-2 genome by reanalyzing the Nanopore
282 RNA-seq data. By searching AAACH (H represents the nucleotide bases A/C/T) on
283 the antisense strand, we found “tgTtt”, “cgTtt” and “agTtt” flanking the TRS motif of
284 *ORF3a*, *E* and *M* at the positions 25402, 26258 and 26494 (**Figure 4C**), respectively,
285 in stead of the “AAGAA-like” motif. In addition, “tgTtt”, “tgTtt”,
286 “ttctT”(“AAGAA-like”) and “tgTtt” were discovered to be closely linked in the gene
287 *S* at the positions 21564, 21570, 21577 and 21579 (**Supplementary 1**), which merits
288 further investigation. The above findings indicated that METTL3 may function in the
289 m6A methylation of sequences flanking the TRS motifs in SARS-CoV-2. Our
290 findings provided clues for the design of more molecular experiments to verify these
291 findings and inferences. The key step leading to the proposal of the arrangement of
292 NSP12-15 and METTL3 (**Figure 4D**) in the global RTC structure was that NSP15
293 cleavage sites are associated to RNA methylation sites. The arrangement of NSP12-15
294 was proposed mainly due to the integration of information from many aspects,
295 particularly considering: (1) the identification of NSP15 cleavage sites in our previous
296 study [18]; (2) TRS hairpins in eight genes (*S*, *E*, *M*, *N*, and *ORF3a*, *6*, *7a* and *8*) are
297 conserved in 292 genomes of betacoronavirus subgroup B; and (3) the motif RRACH

298 (particularly AAACH) on the antisense strand, which was not considered in the
299 previous study [4].

300 By comprehensive analysis of the above results, we proposed that the RTC
301 produces the double-strand RNAs (dsRNAs) and processes single-strand RNAs
302 (ssRNAs) in two routes (**Figure 4D**). RTC functionally starts with NSP13 that
303 unwind template RNAs [7]. In the first route, NSP12 synthesizes RNAs with error
304 correction by NSP14 to produce dsRNAs using gRNAs(+) or gRNAs(-) as templates
305 [21]. The second route processes ssRNAs, which are methylated at internal sites and
306 cleaved by NSP15 for jumping transcription. Then, gRNAs(+) or gRNAs(-) are
307 further in different ways: most gRNAs(+) are packaged and a few continue to be
308 templates for RNA synthesis in the next round, while gRNAs(-) are cleaved for
309 jumping transcription or degradation and the uncleaved ones continue to be templates
310 for RNA synthesis in the next round. This explained the extremely high ratio between
311 sense and antisense reads analyzed in our previous study [10]. The two-route model
312 explained another previous study that demonstrated that knockdown of NSP15 by
313 mutation increases accumulation of viral dsRNA [22]. This is because that
314 knockdown of NSP15 increases the uncleaved gRNAs(-), which continue to be
315 templates for more dsRNA production.

316

317 **Conclusion and Discussion**

318 In the present study, we proposed a two-route model to answer how the RTC
319 functions in the jumping transcription of CoVs and determined the theoretical
320 arrangement of NSP12-15 and METTL3 in the global RTC structure. NSP12-15 and
321 METTL3 form the main structure of the RTC. Based on the available protein structure
322 data, NSP7 and NSP8, acting as the cofactors of NSP12, may be also included in the
323 main structure of the RTC [7]. The results of previous experiments suggest that NSP8
324 is able to interact with NSP15 [20]. Therefore, NSP15 may connect to NSP8 in the

325 global structure of CoV RTC. Our model does not rule out the involvement of other
326 proteins (e.g., ORF8) in the global RTC structure or other proteins in the internal
327 methylation of CoV RNAs. More importantly, our results reveal the associations
328 between multiple functions of the RTC, including NSP15 cleavage, RNA methylation,
329 CoV replication and transcription at the molecular level. Future research needs to be
330 conducted to determine the structures of NSP12&14, NSP12&15, NSP12&METTL3
331 and NSP15&METTL3 complexes by Cryo-EM. These local RTC structures can be
332 used to assemble a global RTC structure by protein-protein docking calculation.
333 Future drug design targeting SARS-CoV-2 needs to consider protein-protein and
334 protein-RNA interactions in the RTC, particularly the complex structure of NSP15
335 with the TRS hairpin.

336

337 **Materials and Methods**

338 The *Betacoronavirus* genus includes five subgenus (*Embecovirus*, *Sarbecovirus*,
339 *Merbecovirus*, *Nobecovirus* and *Hibecovirus*), which are defined as subgroups A, B,
340 C, D and E. 1,265 genome sequences of betacoronaviruses (in subgroups A, B, C and
341 D) were downloaded from the NCBI Virus database
342 (<https://www.ncbi.nlm.nih.gov/labs/virus>) in our previous study [17]. Two genomes
343 (NC_025217 and KY352407) of betacoronaviruses (in subgroup E) were also
344 downloaded. Among 1,265 genomes, 292 belongs to betacoronavirus subgroup B
345 (including SARS-CoV and SARS-CoV-2). 1,178, 480 and 194 genome sequences of
346 Alphacoronavirus, Gammacoronavirus and Deltacoronavirus were downloaded to
347 validate the TRS motifs (**Figure 1**). Nanopore RNA-seq data was downloaded from
348 the website (<https://osf.io/8f6n9/files/>) for reanalysis. Data cleaning and quality
349 control were performed using Fastq_clean [24]. Statistics and plotting were conducted
350 using the software R v2.15.3 with the Bioconductor packages [25]. Protein structure
351 data (PDB: 6X1B, 7BQ7, 7CXN) were used to analyzed NSP15, NSP10&16 and
352 NSP7&8&12&13, respectively. The structures of NSP12-16 were predicted using

353 trRosetta [26]. The minimum free energies (MFEs) of hairpins were estimated by
354 RNAeval v2.4.17 with default parameters.

355

356 **Supplementary information**

357

358 **Declarations**

359 **Ethics approval and consent to participate**

360 Not applicable.

361

362 **Consent to publish**

363 Not applicable.

364

365 **Availability of data and materials**

366 All data used in the present study was download from the public data sources.

367

368 **Competing interests**

369 The authors declare that they have no competing interests.

370

371 **Funding**

372 This work was supported by the Yunnan Applied Basic Research - Yunnan
373 Provincial Science and Technology Department - Kunming Medical University joint
374 projects (Grant No. 202101AY070001-073), National Natural Science Foundation of
375 China (31700787) to Guangyou Duan and National Natural Science Foundation of
376 China (31900444) to Zhi Cheng. The funding bodies played no role in the study
377 design, data collection, analysis, interpretation or manuscript writing.

378

379 **Authors' contributions**

380 Shan Gao conceived the project. Shan Gao and Dong Mi supervised this study.
381 Jianguang Liang, Shunmei Chen, Fan Yang and Zhi Cheng downloaded, managed and
382 processed the data. Guangyou Duan and Jinsong Shi performed programming. Xin Li
383 predicted and analyzed the protein structures. Shan Gao drafted the main manuscript
384 text. Shan Gao and Jishou Ruan revised the manuscript.

385

386 **Acknowledgments**

387 We are grateful for the help from the following faculty members of College of
388 Life Sciences at Nankai University: Wenjun Bu, Tao Zhang, Dawei Huang,
389 Mingqiang Qiao, Yanqiang Liu and Zhen Ye. We would like to thank Editage
390 (www.editage.cn) for polishing part of this manuscript in English language. This
391 manuscript was online as a preprint on Feb 18th, 2021 at
392 <https://biorxiv.org/cgi/content/short/2021.02.17.431652v1>.

393

394 **REFERENCES**

- 395 [1] X. Li, G. Duan, W. Zhang, J. Shi, J. Chen, S. Chen, S. Gao, and J. Ruan. A Furin
396 Cleavage Site Was Discovered in the S Protein of the 2019 Novel Coronavirus.
397 Chinese Journal of Bioinformatics (In Chinese) 2020, 18(2): 103-108.
- 398 [2] G. Duan, J. Shi, Y. Xuan, J. Chen, C. Liu, J. Ruan, S. Gao, and X. Li. 5' UTR
399 Barcode of the 2019 Novel Coronavirus Leads to Insights into Its Virulence. Chinese
400 Journal of Virology (In Chinese) 2020, 36(3): 365-369.
- 401 [3] C. Jiayuan, S.Jinsong , O. Yau Tung, L.Chang, L. Xin, Z.Qiang, R. Jishou, and G.
402 Shan. Bioinformatics Analysis of the 2019 Novel Coronavirus Genome. Chinese
403 Journal of Bioinformatics (In Chinese) 2020, 18(2): 96-102.
- 404 [4] D. Kim, J.-Y. Lee, J.-S. Yang, J.W. Kim, V.N. Kim, and H. Chang. The
405 Architecture of SARS-CoV-2 Transcriptome. Cell 2020, 181(4): 914-921.
- 406 [5] S.J.R. da Silva, C.T. Alves da Silva, R.P.G. Mendes, and L. Pena. Role of
407 nonstructural proteins in the pathogenesis of SARS-CoV-2. J Med Virol 2020, 92:
408 1427-1429.
- 409 [6] Denison MR, Graham RL, Donaldson EF, Eckerle LD, Baric RS. Coronaviruses:
410 an RNA proofreading machine regulates replication fidelity and diversity. RNA Biol.
411 2011, 8(2):270-279.

- 412 [7] L. Yan, Y. Zhang, J. Ge, L. Zheng, Y. Gao, T. Wang, Z. Jia, H. Wang, Y. Huang,
413 M. Li, Q. Wang, Z. Rao, and Z. Lou, Architecture of a SARS-CoV-2 mini replication
414 and transcription complex. *Nature Communications* 2020, 2020(2020): 1-6.
- 415 [8] Y. Kim, R. Jedrzejczak, N.I. Maltseva, M. Wilamowski, M. Endres, A. Godzik, K.
416 Michalska, and A. Joachimiak. Crystal structure of NSP15 endoribonuclease NendoU
417 from SARS-CoV-2. *Protein Science* 2020, 29(7): 1596-1605.
- 418 [9] S.G. Sawicki, and D.L. Sawicki. A New Model for Coronavirus Transcription. in:
419 L. Enjuanes, S.G. Siddell, and W. Spaan, (Eds.). *Coronaviruses and Arteriviruses*,
420 Springer US, Boston, MA, 1998, pp. 215-219.
- 421 [10] Xin Li, Zhi Cheng, Fang Wang, Jia Chang, Qiang Zhao, Hao Zhou, Chang Liu,
422 Jishou Ruan, Guangyou Duan, Shan Gao. A negative feedback model to explain
423 regulation of SARS-CoV-2 replication and transcription. *Frontiers in Genetics* 2021,
424 10: 1-11.
- 425 [11] H.S. Hillen, G. Kokic, L. Farnung, C. Dienemann, and P. Cramer. Structure of
426 replicating SARS-CoV-2 polymerase. *Nature* 2020, 584(7819): 1-6.
- 427 [12] N.E. Grosseohme, L. Li, S.C. Keane, P. Liu, C. Iii, J.L. Leibowitz, and D.P.
428 Giedroc, Coronavirus N Protein N-Terminal Domain (NTD) Specifically Binds the
429 Transcriptional Regulatory Sequence (TRS) and Melts TRS-cTRS RNA Duplexes.
430 *Journal of molecular biology* 394 (2009) 544-557.
- 431 [13] I. Sola, J.L. Moreno, S. Zuniga, S. Alonso, and L. Enjuanes, Role of Nucleotides
432 Immediately Flanking the Transcription-Regulating Sequence Core in Coronavirus
433 Subgenomic mRNA Synthesis. *J Virol* 79 (2005).
- 434 [14] A. Papineau, Y. Berhane, T.N. Wylie, K.M. Wylie, S. Sharpe, and O. Lung,
435 Genome Organization of Canada Goose Coronavirus, A Novel Species Identified in a
436 Mass Die-off of Canada Geese. *Scientific Reports* 9 (2019).
- 437 [15] K.A. Mihindukulasuriya, G. Wu, J.S. Leger, R.W. Nordhausen, and D. Wang,
438 Identification of a novel coronavirus from a beluga whale by using a panviral
439 microarray. *J Virol* 82 (2008) 5084-5088.
- 440 [16] Xin Li, Jia Chang, Shunmei Chen, Liangge Wang, Tung On Yau, Qiang Zhao,
441 Zhangyong Hong, Jishou Ruan, Guangyou Duan and Shan Gao. Genomic feature
442 analysis of betacoronavirus provides insights into SARS and COVID-19 pandemics.
443 *Frontiers Microbiology* 2021, 10: 1-11.
- 444 [17] X. Xu, H. Ji, X. Jin, Z. Cheng, X. Yao, Y. Liu, Q. Zhao, T. Zhang, J. Ruan, W.
445 Bu, Z. Chen, and S. Gao. Using pan RNA-seq analysis to reveal the ubiquitous
446 existence of 5' and 3' end small RNAs. *Frontiers in Genetics* 2019, 10: 1-11.
- 447 [18] Liu C, Chen Z, Hu Y, Ji H, Yu D, Shen W, Li S, Ruan J, Bu W, Gao S.
448 Complemented Palindromic Small RNAs First Discovered from SARS Coronavirus.
449 *Genes* 2018, 9(9): 1-11.
- 450 [19] Yount B , Roberts R , Lindesmith L, et al. Rewiring the severe acute respiratory
451 syndrome coronavirus (SARS-CoV) transcription circuit: Engineering a
452 recombination-resistant genome[J]. *Proceedings of the National Academy of Sciences*
453 of the United States of America, 2006, 103(33) : 12546–12551.

- 454 [20] Lianqi Z , Lei L , Liming Y, et al. Structural and Biochemical Characterization of
455 Endoribonuclease Nsp15 Encoded by Middle East Respiratory Syndrome Coronavirus.
456 *Journal of Virology*, 2018, 92.
- 457 [21] Knoops K, Kikkert M, Worm SHEvd, Zevenhoven-Dobbe JC, van der Meer Y,
458 Koster AJ, et al. (2008) SARS-Coronavirus Replication Is Supported by a
459 Reticulovesicular Network of Modified Endoplasmic Reticulum. *PLoS Biol* 6(9):
460 e226. <https://doi.org/10.1371/journal.pbio.0060226>.
- 461 [22] Xufang Deng, Matthew Hackbart, Robert C. Mettelman, Amornrat O'Brien,
462 Anna M. Mielech, Guanghui Yi, C. Cheng Kao, Susan C. Baker. Coronavirus
463 nonstructural protein 15 mediates evasion of dsRNA sensors and limits apoptosis in
464 macrophages. *Proceedings of the National Academy of Sciences* 2017, 114 (21)
465 E4251-E4260.
- 466 [23] Krafcikova P , Silhan J , Nencka R , et al. Structural analysis of the SARS-CoV-2
467 methyltransferase complex involved in RNA cap creation bound to sinefungin. *Nature*
468 *Communications*, 2020, 11(1):3717.
- 469 [24] M. Zhang, F. Zhan, H. Sun, X. Gong, Z. Fei, and S. Gao. Fastq_clean: An
470 optimized pipeline to clean the Illumina sequencing data with quality control,
471 *Bioinformatics and Biomedicine (BIBM)*, 2014 IEEE International Conference on,
472 IEEE, 2014, pp. 44-48.
- 473 [25] S. Gao, J. Ou, and K. Xiao. R language and Bioconductor in bioinformatics
474 applications(Chinese Edition), Tianjin Science and Technology Translation
475 Publishing Ltd, Tianjin, 2014.
- 476 [26] Yang J, Anishchenko I, Park H, Peng Z, Baker D. Improved protein structure
477 prediction using predicted interresidue orientations. *Proceedings of the National*
478 *Academy of Sciences* 2020, 117(3), 1496-1503.
- 479